RSC Advances

This is an *Accepted Manuscript*, which has been through the Royal Society of Chemistry peer review process and has been accepted for publication.

Accepted Manuscripts are published online shortly after acceptance, before technical editing, formatting and proof reading. Using this free service, authors can make their results available to the community, in citable form, before we publish the edited article. This *Accepted Manuscript* will be replaced by the edited, formatted and paginated article as soon as this is available.

You can find more information about *Accepted Manuscripts* in the Information for Authors.

Please note that technical editing may introduce minor changes to the text and/or graphics, which may alter content. The journal's standard Terms & Conditions and the Ethical guidelines still apply. In no event shall the Royal Society of Chemistry be held responsible for any errors or omissions in this *Accepted Manuscript* or any consequences arising from the use of any information it contains.

ROYAL SOCIETY OF CHEMISTRY

www.rsc.org/advances

Chemical control of struvite scale by a green inhibitor polyaspartic acid

Han Li[1], Sheng-Hui Yu[1], Qi-Zhi Yao[2], Gen-Tao Zhou[1*], Sheng-Quan Fu[3]

[1] CAS Key Laboratory of Crust-Mantle Materials and Environments, School of Earth and Space Sciences, University of Science and Technology of China, Hefei 230026, P. R. China.

[2] School of Chemistry and Materials Science, University of Science and Technology of China, Hefei 230026, P. R. China.

[3] Hefei National Laboratory for Physical Sciences at Microscale, University of Science and Technology of China, Hefei 230026, P. R. China.

● Corresponding author：Prof. Dr. Gen-Tao Zhou

Email: gtzhou@ustc.edu.cn

Tel.: 86 551 63600533

Fax: 86 551 63600533

RSC Advances Accepted Manuscript

Abstract

Many efforts have been made to develop effective chemical inhibitors for struvite scale, which causes a range of operational problems in wastewater treatment industry. Here, the inhibitory capacity of polyaspartic acid (PASP) on the spontaneous precipitation of struvite at pH 9 was investigated. The struvite precipitates were characterized by X-ray diffraction (XRD), field emission scanning electron microscopy (FESEM), and energy dispersive X-ray spectroscopy (EDX). The precipitation experiments dosed with PASP unveiled that PASP is effective in growth inhibition of struvite and its inhibitory capacity is proportional to its concentration, and that PASP also plays a role in the morphological modification of struvite crystals. The effect of several key parameters, including pH, mixing energy, reaction time, and calcium ions on PASP inhibition performance was examined for potentially practical application. The results showed that the inhibitory capacity of PASP is sustainable and efficient. The dissolution experiments dosed with PASP were also performed, and the results showed that PASP can accelerate the dissolution of the preformed struvite, and the capacity increases with its concentration. Therefore, PASP can potentially act as a feasible and environmentally-friendly inhibitor and cleaning agent for struvite scale.

Keywords: Struvite; Ployaspartic acid (PASP); Scale inhibition; Dissolution; Complexation

RSC Advances Accepted Manuscript

1. Introduction

The formation of struvite deposits in wastewater treatment plants (WWTPs) has been widely reported since 1939 when it was first identified in the digested sludge supernatant lines.[1] Struvite, known as magnesium ammonium phosphate hexahydrate ($MgNH_4PO_4 \cdot 6H_2O$), crystallizes in the orthorhombic system and adopts a number of natural morphologies including equant, wedge-shaped, short prismatic, and tabular forms.[2] When the concentrations of magnesium, ammonium and phosphate ions exceed struvite solubility product, its precipitation occurs. The wastewater usually contains large amounts of phosphorus and nitrogen, and about 80 % of N and 50 % of P originate from urine.[3] The anaerobic digestion further solubilizes organic-P and N to PO_4^{3-} and NH_4^+, favoring the formation of struvite.[4-5] Struvite crystals tend to form hard scale on process equipment surfaces of WWTPs, such as sludge liquors pipes, pumps, centrifuges and aerators, leading to clogging and breakdowns of these equipment.[1, 6-7]

In order to eliminate the nuisance, many efforts have been made to deal with the formation of struvite based on four principal approaches. In the first approach, the existing struvite scale is removed by acid washing or chipped away manually with a hammer and a chisel.[8] Obviously, it is a time and manpower consuming maintenance project. The second approach aims at reducing the potential of struvite precipitation by lowering supersaturation level. Initially, the digested sludge stream holding high supersaturation is diluted with secondary effluent to reduce the supersaturation, but the mitigation of struvite formation is proved to be limited in practice.[9-10] Recently, chemical dosing of iron (III) salts is employed as a common method to remove the phosphorus in wastewater.[1, 11] However, this process can produce large amounts of sludge and has poor removal ability.[4, 12] Chemical inhibitors, such as ethylenediaminetetraacetic acid (EDTA), sodium polyphosphate, and silicates, have been also used to reduce the magnesium concentration by forming chelates or less soluble substance with magnesium ions in solution.[1, 11] Among these inhibitors, EDTA

RSC Advances Accepted Manuscript

was tested to be quite efficient but usually degrades slowly in the environment.[11, 13-15] This has raised environmental concerns about its role in heavy metal mobilization in groundwater.[13, 16] For the third approach, the inhibition was achieved by selective binding of the inhibitor molecules with some specific crystal faces of struvite, hence decreasing struvite growth rates. For example, Wierzbicki et al.[17] found that phosphocitrate preferentially binding to (101) faces of struvite leads to morphological modification or total growth cessation of struvite when sufficient phosphocitrate is used. The fourth strategy is to encourage struvite precipitation by adding $MgCl_2$ and NaOH into a specific reactor, as the chemical composition and the pH of wastewaters determine the potential of struvite precipitation.[1, 18-19] In this way, the spontaneous precipitation of struvite can be prevented in the WWTPs.

Among these approaches, the fourth has been a research focus in recent years since this crystallization technique was also regarded as an effective way to recover phosphorus fertilizer.[20-21] However, the disadvantages for this technique are apparent including : (1) Except for the supernatant of digested sludge containing relatively high concentrations of ammonium and phosphate, many wastewater processes cannot fulfill the basic requirement for struvite precipitation.[22] (2) The process has never been proven commercially profitable due to supplementation of magnesium salt and sodium hydroxide.[20, 22] (3) The incorporation of toxic heavy metals, metalloids (e.g., Cr, Zn, and As) and pathogens into struvite crystals can act potentially as a source of pollution when struvite is used as fertilizer.[23-28] (4) In sludge liquors, calcium ion levels can be high relative to magnesium.[29] Calcium ions can interact with phosphate to form hydroxylapatite or amorphous calcium phosphates, leading to the inhibition of struvite production and impurity of the recovered product.[20, 30] (5) Undesired struvite fine particles are often generated in the crystallization processes due to the high mixing energy (or turbulence) needed to suspend the growing particles, resulting in a loss of struvite particles for phosphorus recovery.[31] (6) The fertilization efficiency of struvite is not superior to other phosphate based compounds, such as monocalcium phosphate ($Ca(H_2PO_4)_2 \cdot H_2O$) and dicalcium phosphate ($CaHPO_4 \cdot 2H_2O$).[32] Hence, Hao et al.[32] pointed out that phosphate recovery should not just focus on struvite.

RSC Advances Accepted Manuscript

In view of the harm of struvite scale and the disadvantages of struvite crystallization recovery technique, it is still a challenge to search for effective chemical inhibitors and develop new antiscale techniques. Normally, wastewaters tend to be deficient in magnesium ions.[22] So sequestering magnesium ions will be an ideal way to prevent struvite precipitation. Polyaspartic acid (PASP) is a synthetic polyamino acid and rich in carboxylic functional groups that can combine with metal ions to form metal−PASP species. [16, 33] PASP has been reported to be an effective inhibitor of calcium carbonate, calcium oxalate and calcium phosphate.[34-36] Moreover, PASP is water-soluble, nontoxic, biocompatible, and highly biodegradable, so it is regarded as the most promising green scale inhibitor in industry.[37-38] To the best of our knowledge, however, no research has reported on its scale inhibition to struvite. In the present work, we investigated the inhibitory capacity of PASP on struvite in a dynamic environment. The influence of several physicochemical parameters, including pH, mixing energy, reaction time, and the presence of calcium ions on PASP inhibition performance was systematically investigated. The potential of PASP to dissolve existing struvite scale was also assessed.

2. Materials and methods

2.1. Materials

Magnesium chloride hexahydrate ($MgCl_2 \cdot 6H_2O$), ammonium dihydrogen phosphate ($NH_4H_2PO_4$), ammonium chloride (NH_4Cl), and sodium hydroxide (NaOH) were purchased from Sinopharm Chemical Reagent Co., Ltd, and are of analytical grade. The analytical grade PASP was from Chengdu Ai Keda Chemical Technology Co., Ltd, and the molecular weight is 10000. Deionized water was used in all of the experiments.

2.2. Struvite crystallization

All experiments were conducted at room temperature. A synthetic sludge liquor

RSC Advances Accepted Manuscript

was prepared as described by Doyle et al.[39] Concentrations of 4 mM of magnesium and phosphate were used. As ammonium is always in excess relative to magnesium and phosphate in sludge liquor,[22] ammonium chloride was added to produce an excess of ammonium ions. In a typical synthesis procedure, 0.05 g (0.005 mmol) of PASP and 0.0407 g (0.2 mmol) of $MgCl_2 \cdot 6H_2O$ were dosed to 40 ml of deionized water in a 50-mL beaker under vigorous stirring to form homogeneous solution A. Then, 0.023 g (0.2 mmol) of $NH_4H_2PO_4$ and 0.0214 g (0.6 mmol) of NH_4Cl were dissolved in 10 ml of deionized water to form solution B. Solution B was introduced into solution A under continuous stirring, and a homogeneous synthetic liquor was obtained, with a molar ratio of 1:1:3 (Mg^{2+}:PO_4^{3-}:NH_4^+). Afterwards, the pH of the liquor was adjusted to 9.0 by the addition of 0.5 M NaOH. The beaker was then covered with parafilm to reduce CO_2 interference and NH_3 volatilization, and stirred for 8 h at 360 rpm on a magnetic stirrer. Finally, the product was isolated by centrifugation (1400 g for 3 min), washed with absolute alcohol three times, and dried in vacuum at room temperature for 48 h. The same procedures were employed to study the effect of PASP concentration, reaction time, mixing energy (stirring speed), pH, and Mg/Ca ratio on struvite formation. All trials were conducted in triplicate in our experiments.

2.3. Struvite dissolution

The struvite used for the dissolution was synthesized via homogeneous precipitation by dissolving 0.508 g of $MgCl_2 \cdot 6H_2O$ and 0.288 g of $NH_4H_2PO_4$ in a 50-mL beaker containing 50 ml of deionized water under vigorous stirring. The concentrations of Mg^{2+}, PO_4^{3-}, and NH_4^+ were 50 mM. The pH of this solution was adjusted to 8.0 using 0.25 M NaOH. The beaker was then covered with parafilm and kept static. After aging for 4 h, the product was harvested by the similar way described in Section 2.2. The XRD analysis confirmed that the obtained product was pure struvite (data not shown), and the SEM observation revealed that the struvite crystals exhibited coffin-like shape. The dissolution experiments were conducted at room temperature. 0.05 g of PASP was dissolved to 50 ml of deionized water in a 50-mL beaker, and then the pH was adjusted to 8.0 by using of 0.25 M NaOH. After

RSC Advances Accepted Manuscript

the addition of 50 mg of struvite powder, the beaker was covered with parafilm and stirred for 30 min at 360 rpm on a magnetic stirrer. Finally, the remaining precipitate was collected by the way described in Section 2.2. The same procedures were employed in the PASP concentration-dependent dissolution experiments. All trials were also conducted in triplicate.

2.4. Analytical techniques

X-ray diffraction pattern (XRD) was recorded on an X-ray diffractometer equipped with Cu Kα irradiation (λ = 0.154056 nm, Japan, MapAHF). The morphology and size of the precipitate particles were observed by a field emission scanning electron microscope (FESEM, JEOL JSM-6700F). Energy dispersive X-ray spectroscopy (EDX) analyses of the samples coated with Au were obtained with an EDAX detector installed on the same FESEM.

3. Results and discussion

3.1. Effect of PASP concentration on struvite formation

In order to understand the effect of PASP on struvite crystallization and growth, a series of experiments with the PASP concentration from 0.0 to 0.8 mM were first conducted. The XRD results of the precipitation products confirmed that all of the precipitates obtained with and without PASP are orthorhombic struvite with space group $Pmn2_1$ (JCPDS file of No.15-0762), and the representative XRD patterns are shown in Figure 1a and b. The FESEM results of the struvite precipitates are depicted in Figure 2. It can be seen from Figure 2a that a large number of rod-shaped crystals were obtained in the absence of PASP, with a length of ca. 30 μm and a width of ca. 10 μm. When 0.01 mM of PASP was dosed, the product turned out to be arrowhead-shaped with a reduced length of ca. 5 μm (Figure 2b), which is significantly different from the rod-shaped structure. This morphology was held as PASP concentration was further increased to 0.05 and 0.1 mM. However, as the PASP

RSC Advances Accepted Manuscript

concentration reached 0.3 mM, the panoramic FESEM image shows that massive trapezoidal crystals with a length of ca. 7 μm and less rod-like crystals coexisted (Figure 2c). The further magnified image shows that the "rods" are also trapezoidal (inset in Figure 2c). As PASP concentration raised to 0.5 mM, the products took on three shapes, mainly including trapezoid (ca. 7 μm) and equilateral triangle (ca. 5 μm), and a few rhomboids (ca. 14 μm) (Figure 2d). Further increasing PASP concentration to 0.6 or 0.7 mM did not result in much more change in morphology. In particular, no precipitate could be formed when 0.8 mM of PASP was used. It seems that PASP significantly impacts not only on struvite formation but also on its morphogenesis. Figure 1c quantitively depicts the effect of PASP on struvite precipitate. Figure 1c showed that the struvite mass dramatically decreased with the increase in PASP concentration except for 0.01 mM, indicating that the strong inhibition occurred, and the complete inhibition was achieved with the dose of 0.8 mM PASP. Doyle et al. [11] tested the effectiveness of EDTA on preventing struvite precipitation. According to their study, as much as 8 mM of EDTA is needed to achieve the complete inhibition of struvite precipitation. In this regard, PASP is much more effective than EDTA. Moreover, the size of struvite crystals obtained in the presence of PASP was markedly reduced. This will make struvite easier to be washed away and harder to scale.

It is well known that PASP is a good chelating agent, and can coordinate with a variety of metal cations to form complex species.[16, 33] Therefore, its coordination with Mg^{2+} can be expressed as follows:

$$Mg^{2+} + nPASP \leftrightarrows Mg(PASP)_n \quad (1)$$

$$Mg^{2+} + NH_4^+ + H_2PO_4^- + 6H_2O \leftrightarrows MgNH_4PO_4 \cdot 6H_2O\downarrow + 2H^+ \quad (2)$$

where the coordination and precipitation reactions (1) and (2) compete with each other, and the precipitation will predominate with raising pH based on the reaction (2). With the precipitation of struvite, free Mg^{2+} ions will decrease and the coordination equilibrium will shift towards disassociation of Mg-PASP complexes, leading to the increase of free PASP. The released PASP molecules can selectively bind to crystal faces of struvite, and thus affect the crystal growth habit (e.g., Figure 2). Therefore, PASP molecules play the dual roles during the scale inhibition: morphological

RSC Advances Accepted Manuscript

modification and precipitation inhibition of struvite. In fact, the similar arrowhead-shaped struvite has been observed in the presence of PASP in our previous biomimetic mineralization experiments,[40] and the selective recognition and binding of PASP onto {010} and {101} faces of struvite crystals were believed to be responsible for the formation of the specific morphology. Because these faces have a high density of magnesium cations, and hence provide a positively charged environment for the preferential adsorption and binding of PASP molecules rich in negatively charged carboxyl side chains.[17, 40-41] PASP molecules binding to these faces decrease their growth rate and lead to an enhanced expression of these faces, thus modifying crystal morphology. Similarly, trapezoid and equilateral triangle observed in our case may also result from the preferential adsorption and binding of PASP onto some specific faces of struvite crystals. As for the increase of struvite precipitate at 0.01 mM of PASP, it is possible because less PASP molecules in the liquor cannot cause a significant decrease in free Mg^{2+} by their complexation with Mg^{2+} ions. In contrast, the low concentration of PASP can induce Mg^{2+} and NH_4^+ aggregation and accumulation around them by their carboxylic groups, and promote struvite nucleation. As a result, the less PASP molecules in the liquor act as a nucleation template, and thus facilitate the precipitation of struvite.[42] The similar effect has also been reported by Elhadj et al.[43] in the system of PASP and calcite. Nevertheless, with the increase of PASP concentration, the coordination between PASP and Mg^{2+} predominates over the template function of PASP. Therefore, high concentration of PASP can effectively block struvite precipitation and growth, even completely avoid the formation of struvite precipitate.

3.2. Effect of reaction conditions on PASP inhibition performance

The influence of several key parameters, including reaction time, mixing energy, pH, and calcium ions on the scale inhibition performance of PASP was examined. A 0.5 mM of PASP was dosed for each run to guarantee an effective and incomplete inhibition of struvite formation, and other conditions were the same as the PASP concentration-dependent experiments.

RSC Advances Accepted Manuscript

3.2.1. Reaction time

If PASP was used as an inhibitor to prevent struvite formation in WWTPs, its inhibitory capacity should last enough time to allow wastewater pass through the whole pipes before precipitation. Hence, the experiments with stirring time of 8, 16, 24, 48 h were carried out. The precipitates were always formed at different time intervals due to the limited dose of PASP (0.5 mM). The XRD analyses confirmed that these precipitates were also struvite (e.g., Figure 1b). The FESEM results showed that the morphology and size of struvite obtained after 16, 24, and 48 h were the same as the 8-hour product (e.g., Figure 2d). It seems that the different stirring time have no effect on the precipitate phase and morphology. Figure 3a shows the plot of precipitate mass versus stirring time. Although the slight increase in precipitate mass was observed from 8 to 16 h, the precipitate mass almost remained constant after 16 h of stirring, indicating that the magnesium-PASP species are stable. Therefore, PASP inhibition performance is effective and sustainable in a longer period of time, ensuring wastewater to be treated with less struvite precipitation.

3.2.2. Mixing energy

It is commonly observed that struvite preferentially accumulates in specific locations of a treatment or conveyance system with high mixing energy, such as pipe elbows, pumps, and mixers, rather than uniform deposition.[44] The mechanisms responsible for the preferential accumulation of struvite are associated with the mixing energy (or turbulence). In the areas of high mixing energy, CO_2 liberation is enhanced. This can increase pH of the solution, and therefore favor the formation of struvite crystals.[20] More importantly, struvite growth rate was found to be transport-limited.[44] High mixing energy will enhance the mass transfer of solute to the crystals and facilitate struvite crystallization and growth.[44-45] In our experiments, we tested the effect of mixing energy on PASP inhibition performance. The stirring speed ranged from 0 to 960 rpm (i.e., 0, 120, 360, 600, 960 rpm). After 8 h of reaction, no product was obtained in the static experiment (0 rpm) and the solution was always

RSC Advances Accepted Manuscript

clear. In contrast, the struvite crystals with similar morphology and size were harvested under magnetic stirring ranging from 120 to 960 rpm (e.g., Figure 1a and 2d), revealing that the stirring favors the nucleation and growth of struvite. However, no marked changes in precipitate mass were observed with the increase in stirring speed (Figure 3b), further indicating that in the presence of PASP, the high mixing energy cannot also transport enough free Mg^{2+} to the growth fronts of struvite crystals, and thereby accelerate crystal growth. In other words, the high mixing energy cannot weaken the inhibitory capacity of PASP, and PASP can be potentially applied to controlling struvite scaling at different locations, especially those high-mixing environments.

3.2.3. Initial pH

The pH can affect dissolution and supersaturation, as well as morphology, particle size, and purity of struvite.[20, 46] The wastewater may have different pH values depending on the type and source, and the pH cannot be always controlled or maintained throughout struvite crystallization process.[46] Therefore, the effect of initial pH (pH_i) on PASP performance was investigated. Here, the pH_i ranged from 8 to 11 (i.e., 8, 9, 10, 11). The control experiments without PASP were also conducted. In the absence of PASP, the collected precipitates all were the rod-shaped struvite at pH_i 8-10 (Figure 1a and 2a, Figure S1a,b and S2a); At pH_i 11, the precipitate consists of the rod-shaped struvite and plate-like cattiite [$Mg_3(PO4)_2 \cdot 22H_2O$], which were confirmed by the XRD and EDX analyses (Figure S1c and S2b, S3a and b). In the presence of PASP, no precipitate was obtained at pH_i 8, but pure struvite was formed at pH_i 9-11 (Figure 1a, Figure S1d and e), and these struvite crystals gets slenderer with pH_i (Figure 2d, Figure S2c and d). The variation trend of struvite shape agrees well with the results reported by Ma et al.[46] This is because high precipitation rate and changes in aqueous speciation decrease the concentrations of Mg^{2+}(aq), NH_4^+(aq), and PO_4^{3-}(aq), resulting in the limiting of crystal growth at higher pH_i.[46] Figure 3c shows the effect of pH_i on the mass of precipitate products in the presence of 0.0 and 0.5 mM PASP. It can be seen that the variation trends are similar under the two conditions.

RSC Advances Accepted Manuscript

That is, the mass increased with pH_i, and the highest at pH_i 10. This is consistent with the previous observations by Ma and Rouff.[24] The increase in yield with pH_i can be attributed to an increase in the activity of PO_4^{3-}(aq) as pH increase promotes the equilibrium shifting from $H_2PO_4^-$ and HPO_4^{2-} to PO_4^{3-}species. However, at pH_i 11, this effect is neutralized by the reduced activity of NH_4^+(aq) due to increased formation of NH_3 species, and by the hydrolysis of Mg^{2+}(aq) to $MgOH^+$(aq).[24] It is notable that in the presence of PASP, the precipitation of struvite was significantly inhibited at pH_i from 8 to 11 compared with the controls (Figure 3c). Therefore, PASP can inhibit struvite growth over a large pH_i range, and additional dose of PASP can achieve the same inhibitory efficiency at higher pH_i.

3.2.4. Mg/Ca ratio

In sludge liquors, calcium levels can be high relative to magnesium.[29] These calcium ions can interact with phosphate or carbonate ions to form additional mineral precipitates, such as hydroxylapatite and calcite.[20] In this context, struvite formation can be inhibited if the supply of phosphate is limited. As a chelating agent, PASP can form stable complexes with calcium and magnesium ions in solution.[16, 33] The presence of calcium ions will unavoidably reduce the inhibitory efficiency of PASP on struvite. Therefore, the inhibitory experiments at Mg/Ca ratios of 1:0, 2:1, 1:1, and 1:2 were performed. Similarly, the precipitates were examined by FESEM and XRD techniques. In the absence of PASP, the precipitates exhibited different mineralogical characteristics over the range of Mg/Ca ratios. Without the addition of Ca, the pure rod-shaped struvite was obtained (Figure 1a and 2a). When the Mg/Ca ratio was 2:1, the rod-shaped crystals coated with nanoparticles and irregular aggregates of nanoparticles were formed (Figure S4a). The XRD pattern, despite slight background noises, could still well be indexed as struvite (Figure 4a). Therefore, the rod-like crystals can be safely assigned to struvite, whereas the nanoparticles and their aggregates may be an amorphous precipitate. Further increasing Ca concentration (Mg/Ca = 1:1) led to the enhanced output of irregular aggregates with a few rod-like crystals (Figure S4b), and the much more noises can be observed from its XRD

RSC Advances Accepted Manuscript

pattern (Figure 4b), indicative of the formation of much amorphous matter. When the Mg/Ca ratio reached 1:2, only the huge tabular aggregates were harvested (Figure S4c), and XRD analysis confirmed that the aggregates exhibited an amorphous feature (Figure 4c), indicating that Ca^{2+} present in the liquor facilitate the formation of amorphous precipitate. To further understand the chemical nature of the amorphous aggregates, EDX analyses were also conducted (Figure S3c-g). Combined with the FESEM images and XRD patterns, the aggregates were identified as amorphous calcium phosphate. Le Corre et al. [29] also obtained amorphous calcium phosphate when they studied the impact of calcium on struvite growth. We also found that the addition of Ca inhibited struvite growth but increases the total yield of the precipitates, i.e., the formation of other scales (Figure 3d). However, in the presence of 0.5 mM PASP, only trapezoidal and rod-like struvite was obtained at different Mg/Ca ratios, and no calcium precipitate was harvested (Figure S4d-f, Figure 4d-f). It indicated that calcium ions had priority to complex with PASP, resulting in the decrease of PASP inhibition performance on struvite formation. Therefore, a slight increase in struvite mass was observed with increasing calcium concentration (Figure 3d). However, the mass of struvite obtained in the presence of PASP was still pretty low at different Mg/Ca ratios compared with the experiments without PASP. That is to say, the effect of calcium on PASP inhibition performance was limited and PASP can still exert significant scale inhibition even in the presence of calcium.

3.3. Effect of PASP concentration on struvite dissolution

Except for the inhibition of scale formation, the removal of existing struvite scale is another important work in WWTPs. Investigators have tried to find out effective and environmentally safe chelating agents to provide a feasible alternative to acid dissolution, which can cause corrosion in metallic process equipment and piping systems.[47] The previous studies demonstrate that PASP can promote the dissolution of calcium oxalate and calcium phosphate due to its ability to chelate metal ions in solution.[47-49] Therefore, the chelation of PASP with magnesium may also be a driving force for struvite dissolution. Here, the dependence of struvite dissolution on PASP

RSC Advances Accepted Manuscript

concentration was examined at pH 8. Figure 5 presents the FESEM images of the products before and after dissolution with different concentrations of PASP. The pristine struvite crystals take a coffin-like shape with a length of ca. 30 μm and a width of ca. 10 μm, and a number of tiny pits and crevices can be seen on lateral sides (Figure 5a). After dispersed in the deionized water for 30 minutes, some tiny pits or crevices were enlarged, but the basic configuration still remained, indicating that the limited dissolution occurred (Figure 5b). Although struvite solubility is low in water, it can be 18 mg·100 mL^{-1} at 25 ºC.[20] That is to say, as much as 9 mg of struvite will be dissolved if the dissolution equilibrium is achieved in our case (50 mg struvite + 50 ml of deionized water). Our dissolution experiment revealed that 8.3 mg (16.6%) of struvite was dissolved in deionized water, approaching to the equilibrium dissolution value (Figure S5). When 0.1 mM of PASP was dosed, the struvite crystals became thinner, containing many grooves and deep carvings (Figure 5c). Noticeably, a couple of enlarged corrosion pits could be seen on the surfaces. Some struvite crystals had decreased width and approximately 28.1 mg (56.2%) of struvite was dissolved (Figure S5). Therefore, the dose of PASP can effectively enhance struvite dissolution. As the PASP concentration was 0.5 mM, more remarkable dissolution occurred, resulting in the much thinner morphology, i.e., dumbbell-shaped (Figure 5d). Consistently, over 44 mg (88%) of struvite was dissolved in this case (Figure S5). Hence, the effectiveness of PASP to promote struvite dissolution was proportional to its concentration. Wu and Grant [16] reported that all the carboxyl groups of PASP will be ionized above pH 6, leading to the strongest complexation with magnesium. The complexation reduced the amount of free magnesium ions and therefore broke down the precipitation-dissolution equilibrium, resulting in the enhancement of struvite dissolution (Eq. 2). With increasing PASP concentrations, more complexation will be formed, further promoting the dissolution. Therefore, PASP can be an effective cleaning agent for the existing struvite scale.

4. Conclusions

RSC Advances Accepted Manuscript

In summary, the precipitation experiments dosed with PASP showed that PASP can not only effectively inhibit the formation and growth of struvite, but also significantly change struvite morphology, leading to the evolution from rod-shape to arrowhead-shape, triangle, or trapezoid. Moreover, several key parameters that possibly effect on PASP inhibition performance were also tested, and the results revealed that PASP can still exert strong antiscaling on struvite even in a long running time and a large range of mixing energy. Nevertheless, its inhibition potency is pH dependant, and decreases with pH_i. The presence of calcium ions slightly reduced the inhibition potency of PASP while the dose of PASP prevented the formation of amorphous calcium phosphate. The dissolution experiments dosed with PASP showed that PASP can promote the dissolution of the preformed struvite and the effectiveness increases with its concentration. It appears that PASP has a strong ability to not only effectively inhibit the formation and growth of struvite, but also facilitate struvite dissolution. Therefore, PASP can serve as an environmentally friendly scale inhibitor and scale cleaning agent.

Acknowledgements

This work was partially supported by the Chinese Ministry of Science and Technology (No. 2014CB846003), the Natural Science Foundation of China (No. 41372053), and the Specialized Research Fund for the Doctoral Program of Higher Education (No. 20133402130007).

Electronic supplementary information (ESI)

The characterizations of the samples precipitated at different pH_i and different Mg/Ca ratios, including XRD patterns, FESEM images, and EDX spectra. Plot of remaining mass in the dissolution experiments.

RSC Advances Accepted Manuscript

References

1. J. D. Doyle and S. A. Parsons, *Water Res.*, 2002, **36**, 3925-3940.
2. F. Abbona and R. Boistelle, *J. Cryst. Growth*, 1979, **46**, 339-354.
3. C. Beal, T. Gardner, W. Ahmed, C. Walton and D. Hamlyn-Harris, in Proceedings of AWA Conference, 2007, pp. 1–8.
4. D. Mamais, P. A. Pitt, Y. W. Cheng, J. Loiacono and D. Jenkins, *Water Environ. Res.*, 1994, **66**, 912-918.
5. C. M. Mehta and D. J. Batstone, *Water Res.*, 2013, **47**, 2890-2900.
6. Mohajit, K. K. Bhattarai, E. P. Taiganides and B. C. Yap, *Biol. Wastes*, 1989, **30**, 133-147.
7. J. D. Doyle, K. Oldring, J. Churchley and S. A. Parsons, *Water Res.*, 2002, **36**, 3971-3978.
8. S. Williams, *Environ. Technol.*, 1999, **20**, 743-747.
9. J. Borgerding, *J. Water Pollut. Control Fed.*, 1972, **44**, 813-819.
10. S. A. Parsons and J. D. Doyle, *Water Sci. Technol.*, 2004, **49**, 177-182.
11. J. D. Doyle, K. Oldring, J. Churchley, C. Price and S. A. Parsons, *J. Environ. Eng-Asce*, 2003, **129**, 419-426.
12. K. Fytianos, E. Voudrias and N. Raikos, *Environ. Pollut.*, 1998, **101**, 123-130.
13. J. L. Means, T. Kucak and D. A. Crerar, *Environ. Pollut. B*, 1980, **1**, 45-60.
14. V. Sykora, P. Pitter, I. Bittnerova and T. Lederer, *Water Res.*, 2001, **35**, 2010-2016.
15. J. Prywer and M. Olszynski, *J. Cryst. Growth*, 2013, **375**, 108-114.
16. Y. T. Wu and C. Grant, *Langmuir*, 2002, **18**, 6813-6820.
17. A. Wierzbicki, J. D. Sallis, E. D. Stevens, M. Smith and C. S. Sikes, *Calcified Tissue Int.*, 1997, **61**, 216-222.
18. I. Stratful, M. D. Scrimshaw and J. N. Lester, *Water Res.*, 2001, **35**, 4191-4199.
19. Y. Ueno and M. Fujii, *Environ. Technol.*, 2001, **22**, 1373-1381.
20. K. S. Le Corre, E. Valsami-Jones, P. Hobbs and S. A. Parsons, *Crit. Rev. Env. Sci. Tec.*, 2009, **39**, 433-477.

RSC Advances Accepted Manuscript

21. C. C. Wang, X. D. Hao, G. S. Guo and M. C. M. van Loosdrecht, *Chem. Eng. J.*, 2010, **159**, 280-283.
22. L. E. de-Bashan and Y. Bashan, *Water Res.*, 2004, **38**, 4222-4246.
23. L. Decrey, K. M. Udert, E. Tilley, B. M. Pecson and T. Kohn, *Water Res.*, 2011, **45**, 4960-4972.
24. N. Ma and A. A. Rouff, *Environ. Sci. Technol.*, 2012, **46**, 8791-8798.
25. A. A. Rouff, *Environ. Sci. Technol.*, 2012, **46**, 12493-12501.
26. J. R. Lin, N. Chen and Y. M. Pan, *Environ. Sci. Technol.*, 2013, **47**, 12728-12735.
27. J. R. Lin, N. Chen and Y. M. Pan, *Environ. Sci. Technol.*, 2014, **48**, 6938−6946.
28. A. A. Rouff and K. M. Juarez, *Environ. Sci. Technol.*, 2014, **48**, 6342-6349.
29. K. S. Le Corre, E. Valsami-Jones, P. Hobbs and S. A. Parsons, *J. Cryst. Growth*, 2005, **283**, 514-522.
30. X. D. Hao, C. C. Wang, L. Lan and M. C. M. van Loosdrecht, *Water Sci. Technol.*, 2008, **58**, 1687-1692.
31. K. S. Le Corre, E. Valsami-Jones, P. Hobbs, B. Jefferson and S. A. Parsons, *Water Res.*, 2007, **41**, 419-425. 已后移
32. X. D. Hao, C. C. Wang, M. C. M. van Loosdrecht and Y. S. Hu, *Environ. Sci. Technol.*, 2013, **47**, 4965-4966.
33. S. D. Jiang, Q. Z. Yao, G. T. Zhou and S. Q. Fu, *J. Phys. Chem. C*, 2012, **116**, 4484-4492.
34. X. X. Sheng, M. D. Ward and J. A. Wesson, *J. Am. Chem. Soc.*, 2003, **125**, 2854-2855.
35. A. Bigi, B. Bracci, S. Panzavolta, M. Iliescu, M. Plouet-Richard, J. Werckmann and D. Cam, *Cryst. Growth Des.*, 2004, **4**, 141-146.
36. B. Njegic-Dzakula, L. Brecevic, G. Falini and D. Kralj, *Cryst. Growth Des.*, 2009, **9**, 2425-2434.
37. D. Hasson, H. Shemer and A. Sher, *Ind. Eng. Chem. Res.*, 2011, **50**, 7601-7607.
38. K. L. Dziak and O. Akkus, J. Bone Miner. Metab., 2008, 26, 569-575.
39. J. D. Doyle, R. Philp, J. Churchley and S. A. Parsons, *Process Saf. Environ. Protect.*, 2000, **78**, 480-488.

RSC Advances Accepted Manuscript

40. H. Li, Q. Z. Yao, Y. Y. Wang, Y. L. Li and G. T. Zhou, *Sci. Rep.*, 2015, **5**, No.7718.

41. Z. Romanowski, P. Kempisty, J. Prywer, S. Krukowski and A. Torzewska, *J. Phys. Chem. A*, 2010, **114**, 7800-7808.

42. J. Roque, J. Molera, M. Vendrell-Saz and N. Salvado, *J. Cryst. Growth*, 2004, **262**, 543-553.

43. S. Elhadj, E. A. Salter, A. Wierzbicki, J. J. De Yoreo, N. Han and P. M. Dove, *Cryst. Growth Des.*, 2006, **6**, 197-201.

44. K. N. Ohlinger, T. M. Young and E. D. Schroeder, *J. Environ. Eng-Asce*, 1999, **125**, 730-737.

45. D. Kim, J. Kim, H. D. Ryu and S. I. Lee, *Bioresour. Technol.*, 2009, **100**, 74-78.

46. N. Ma, A. A. Rouff and B. L. Phillips, *ACS Sustain. Chem. Eng.*, 2014, **2**, 816-822.

47. F. Littlejohn, C. S. Grant, Y. L. Wong and A. E. Saez, *Ind. Eng. Chem. Res.*, 2002, **41**, 4576-4584.

48. F. Poumier, P. Schaad, Y. Haikel, J. C. Voegel and P. Gramain, *J. Biomed. Mater. Res.*, 1999, **45**, 92-99.

49. S. W. Guo, M. D. Ward and J. A. Wesson, *Langmuir*, 2002, **18**, 4284-4291.

RSC Advances Accepted Manuscript

Figure captions

Figure 1 Typical XRD patterns of the precipitates from the artificial liquor dosed with 0 (a) and 0.5 (b) mM PASP. (c) Effect of PASP concentration on mass of struvite precipitation. All of the precipitation runs were performed at pH_i 9.0 for 8 h.

Figure 2 FESEM images of the 8 h struvite crystals from the artificial liquor dosed with 0 (a), 0.01 (b), 0.3 (c), and 0.5 (d) mM of PASP.

Figure 3 Mass of the precipitates obtained under different precipitation conditions: (a) different time intervals; (b) different stirring speeds; (c) different pH_i values; (d) different Mg/Ca ratios.

Figure 4 XRD patterns of the precipitates at Mg/Ca ratio 2:1 (a), 1:1 (b), 1:2 (c) dosed with 0 mM PASP, and at Mg/Ca ratio 2:1 (d), 1:1 (e), 1:2 (f) dosed with 0.5 mM PASP.

Figure 5 FESEM images of struvite crystals before (a) and after (b) 30 min of dissolution dosed with 0 (b), 0.1 (c), and 0.5 (d) mM of PASP.

RSC Advances Accepted Manuscript

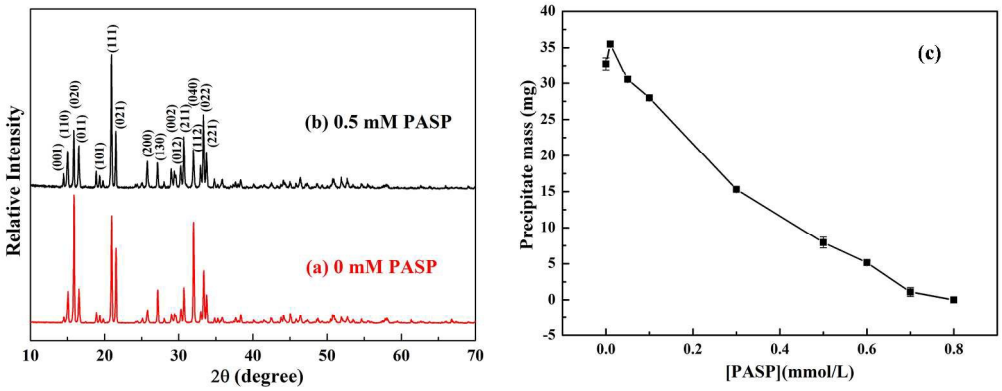

Figure 1

RSC Advances Accepted Manuscript

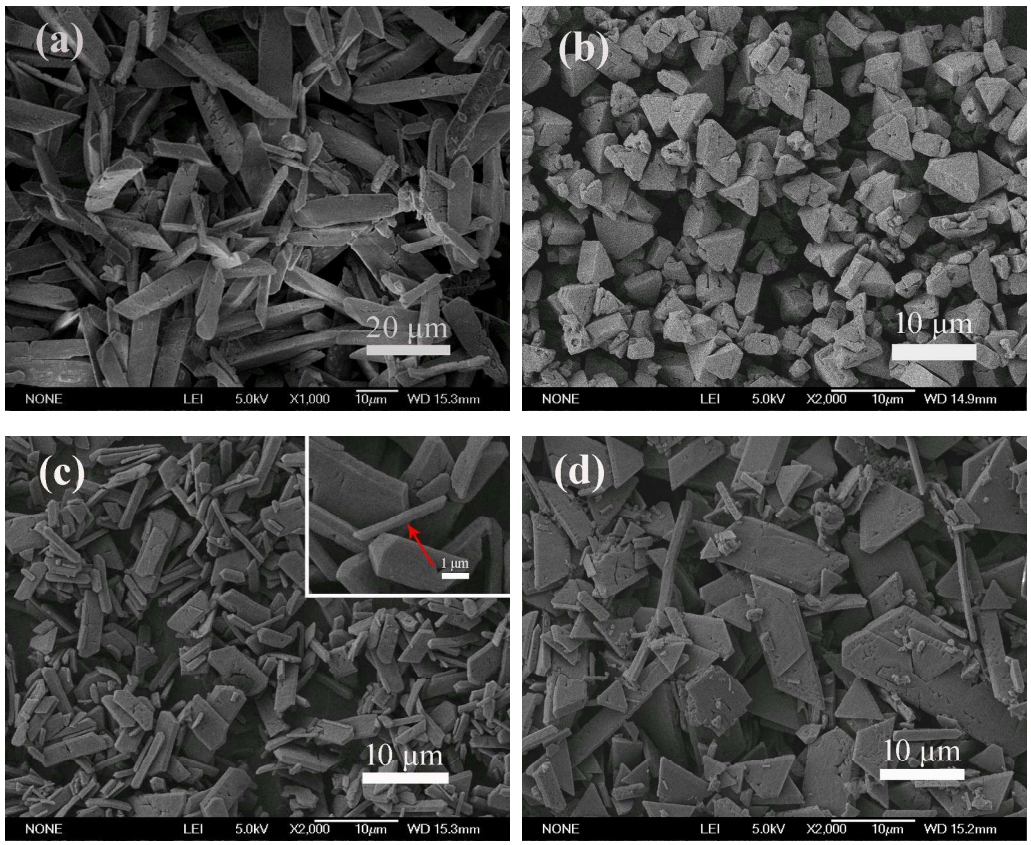

Figure 2

RSC Advances Accepted Manuscript

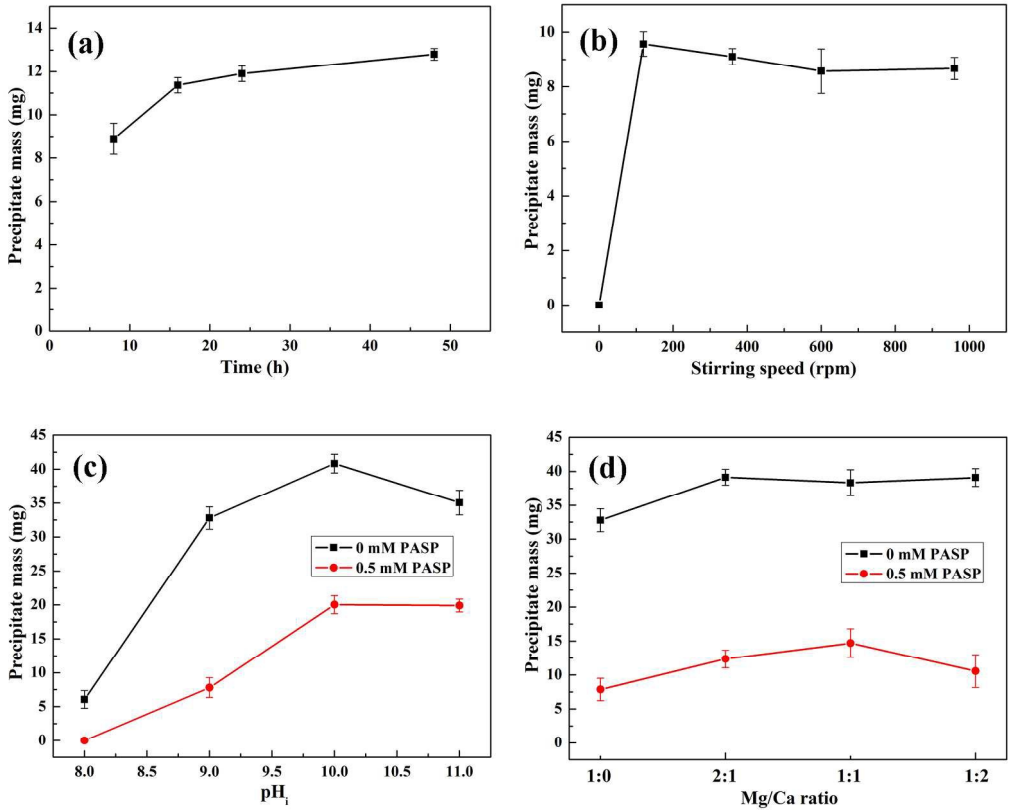

Figure 3

RSC Advances Accepted Manuscript

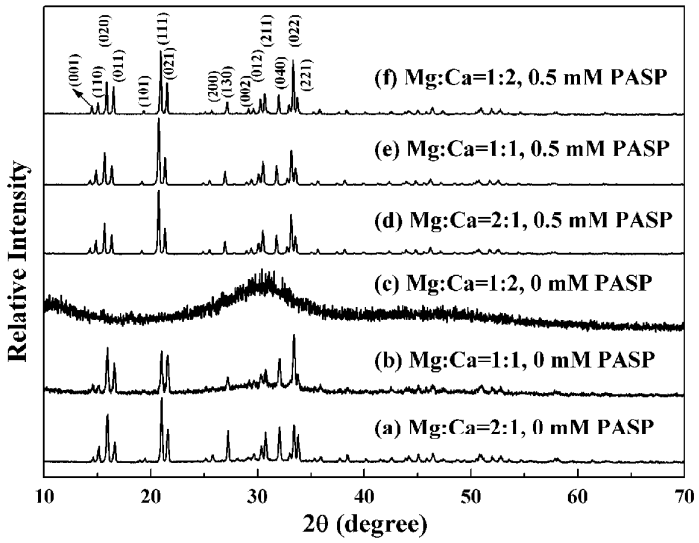

Figure 4

RSC Advances Accepted Manuscript

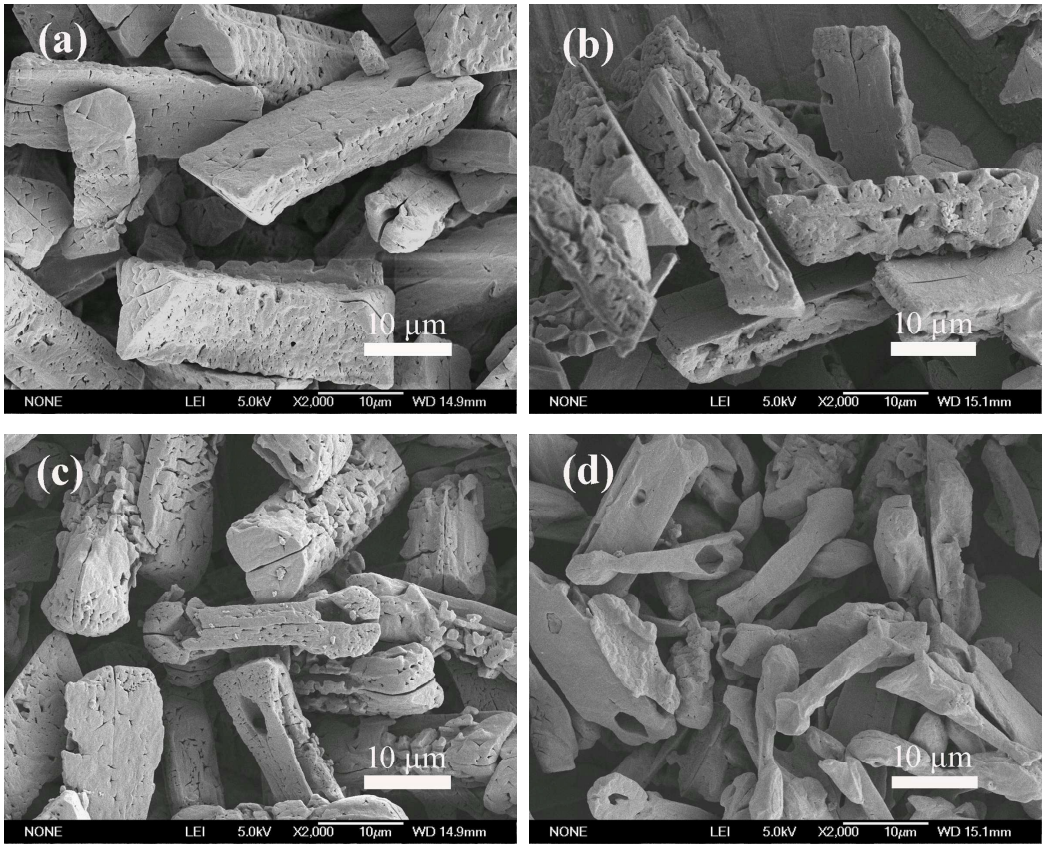

Figure 5

RSC Advances Accepted Manuscript